

# Coupling of Probe Reorientation Dynamics and Rotor Motions to Polymer Relaxation As Sensed by Second Harmonic Generation and Fluorescence

Jacob C. Hooker<sup>†</sup> and John M. Torkelson<sup>\*,‡</sup>

Department of Materials Science and Engineering and Department of Chemical Engineering, Northwestern University, Evanston, Illinois 60208-3120

Received May 22, 1995; Revised Manuscript Received August 31, 1995<sup>®</sup>

**ABSTRACT:** The coupling of various rotational motions of the rotor probes 4-(tricyanovinyl)-*N*-(2-hydroxyethyl)-*N*-ethylaniline (TC1) and julolidenemalononitrile (JMN) to the relaxation dynamics of poly(ethyl methacrylate), poly(isobutyl methacrylate), and an isobutyl methacrylate–TC1 labeled methacrylate copolymer has been investigated by second harmonic generation (SHG) and steady-state fluorescence in both the glassy and rubbery states. In the rubbery state, the temperature dependence of the average rotational reorientation relaxation times,  $\langle\tau\rangle$ , of TC1, both doped and labeled, determined from SHG measurements can be fitted well to the WLF equation with reasonable  $C_1$  and  $C_2$  parameters, indicating coupling to the  $\alpha$ -relaxation in these polymer systems. The value of  $\langle\tau\rangle$  at the glass transition temperature and the weaker temperature dependence of  $\langle\tau\rangle$  in the glassy state also support the conclusion of coupling to the  $\alpha$ -relaxation. However, from fluorescence measurements a much weaker temperature dependence is observed for the smaller scale motions involving internal rotations and/or isomerizations of the acceptor and/or donor moieties on TC1 and JMN, indicating significant decoupling from the  $\alpha$ -relaxation. The decoupling of these internal probe motions from the  $\alpha$ -relaxation mechanism is discussed in terms of  $x$ , a probe-dependent parameter introduced by Loutfy, and  $\xi$ , a parameter described by Ehlich and Sillescu as indicating the degree of coupling to the  $\alpha$ -relaxation. A consideration of the time scales and activation energies associated with the smaller scale, internal rotation of these various moieties suggests at least some coupling to sub- $\beta$ -relaxations. We also note the importance of carefully considering the results of a WLF fit in order to interpret appropriately the nature of the probe coupling to the polymer relaxation.

## Introduction

There have been substantial advances in the use of molecular probe spectroscopy<sup>1,2</sup> for investigating mechanisms associated with complex relaxation behavior in amorphous polymer systems. The molecular probe spectroscopy approaches recently employed include dielectric,<sup>3–7</sup> electron spin resonance,<sup>8,9</sup> nuclear magnetic resonance,<sup>10</sup> UV–visible absorbance (photochromism),<sup>11–13</sup> steady-state fluorescence,<sup>14–21</sup> fluorescence anisotropy decay,<sup>22,23</sup> and photobleaching<sup>23</sup> techniques. Each of these techniques is sensitive to the rotational reorientation or isomerization of all or part of a probe molecule, which in turn is affected by the relaxation processes of its local polymeric environment. Additionally, studies of probe translational motions in polymers have been performed using forced Rayleigh scattering<sup>24</sup> and fluorescence nonradiative energy transfer.<sup>25</sup>

Of particular interest is a class of mobility-sensitive intramolecular charge transfer fluorescence chromophores known as molecular “rotor” probes. These rotor probes have been studied extensively in solution and in bulk amorphous polymers by Loutfy and Law<sup>18,19</sup> and more recently by Royal and Torkelson.<sup>14</sup> In these studies (dialkylamino)malononitriles were used as rotor probes. After absorbing light and being elevated to singlet excited states, these probes have two major pathways for returning to the ground state. The preferred deactivation route is a nonradiative internal conversion mechanism involving bond rotations in the probe. Hindering these rotations causes the probes to

deactivate by emitting a photon or fluorescing. Therefore, the probe fluorescence intensity, quantum efficiency, and excited-state lifetime increase when the local mobility decreases or the local environmental relaxation processes slow down.

Royal and Torkelson<sup>14</sup> demonstrated that rotor probes can be excellent sensors of complex relaxation phenomena in amorphous polymers as they can sense relative rates of physical aging as a function of temperature, the attainment of equilibrium during physical aging on time scales equivalent to those obtained by enthalpy relaxation measurements, bulk-like “asymmetry” behavior, and “memory effects” after multiple temperature jumps. A related study<sup>26</sup> demonstrated quantitative sensitivity of rotor probe fluorescence to plasticization, in particular water sorption and diffusion in a variety of polymeric matrices. Thus, it is clear that there is substantial coupling between rotor probe and polymer dynamics. However, the nature of this coupling has yet to be determined. Through his arguments of sensitivity to free volume, Loutfy<sup>18</sup> proposed that the fluorescence behavior of these probes should follow a Williams–Landel–Ferry (WLF) type temperature dependence.<sup>27</sup> If this were correct, it would imply that the rotational motions associated with the deactivation in these probes would be coupled exclusively to the cooperative segmental motions associated with the polymer  $\alpha$ -relaxation process. However, the fact that there is excellent agreement between the relaxation time scales to achieve equilibrium exhibited by these probes and by bulk enthalpy relaxation measurements during physical aging argues against this conclusion as enthalpy relaxation should be sensitive to all conformational relaxations in the polymer,<sup>28</sup> not just those associated with the  $\alpha$ -relaxation process. (The relatively small size of the internal rotational relaxation processes of the rotor probes may not allow for exclusive coupling to the

\* To whom correspondence should be addressed.

<sup>†</sup> Department of Materials Science and Engineering.

<sup>‡</sup> Department of Chemical Engineering.

<sup>®</sup> Abstract published in *Advance ACS Abstracts*, October 15, 1995.

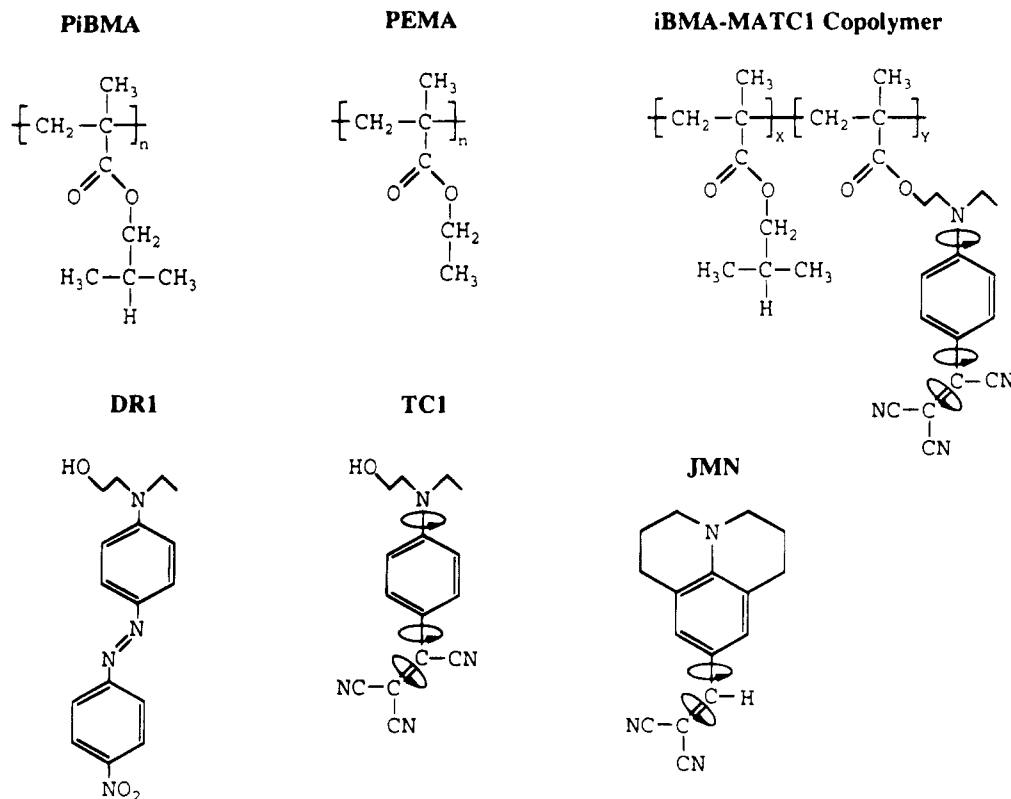


Figure 1. Structures of polymers and chromophores used in this study.

cooperative segmental motions associated with the  $\alpha$ -relaxation, as admitted by Law and Loutfy<sup>19b</sup>.)

Recently, in a new approach for measuring the temporal decay of second-order nonlinear optical properties in doped, poled polymers over nearly 12 orders of magnitude in time, Dhinojwala et al.<sup>6,7,29,30</sup> demonstrated that the rotational reorientation of an entire intramolecular charge transfer molecule such as Disperse Red 1 and (*N,N*-dimethylamino)nitrostilbene is coupled to the  $\alpha$ -relaxation process both above and below the glass transition temperature,  $T_g$ , in polymers such as poly(isobutyl methacrylate), poly(ethyl methacrylate), and polystyrene. In particular, at  $T_g$ , the average rotational reorientation relaxation time,  $\langle\tau\rangle$ , of these second harmonic generation (SHG) chromophores is on the order of 100 s, in agreement with expectations for the average  $\alpha$ -relaxation time at  $T_g$  in both low molecular weight and polymeric glass formers.<sup>28</sup> Above  $T_g$ , the temperature dependence of  $\langle\tau\rangle$  follows that of the WLF equation, with physically meaningful values for the WLF parameters. Below  $T_g$ , the temperature dependence of  $\langle\tau\rangle$  deviates from the WLF fit to the data above  $T_g$ , yielding a much lower temperature dependence which can be described approximately by an Arrhenius fit, with an apparent activation energy of 45–50 kcal/mol, again in agreement with expectations for an  $\alpha$ -relaxation process below  $T_g$ .<sup>31</sup>

The intramolecular charge transfer character of the fluorescence rotor probes also makes them good candidates for use as SHG probes. Given this set of circumstances, the present study focuses on providing data on both the fluorescence behavior and SHG characteristics of rotor probes such as julolidenemalononitrile and 4-(tricyanovinyl)-*N*-(2-hydroxyethyl)-*N*-ethylaniline in poly(alkyl methacrylates) above and below  $T_g$ . As such, this study provides the first comparison between different rotational reorientation processes, in one case the rotation of a moiety on the rotor probe and in the second

the rotational reorientation of the whole molecule, using the same probe/polymer systems. Hence, this study allows for a detailed investigation of the coupling of the rotational/reorientational probe motions to polymer dynamics. In addition, the effects of covalently attaching the chromophore to the polymer on the coupling between probe and polymer dynamics will also be described.

## Experimental Section

**Materials.** Poly(isobutyl methacrylate) (PiBMA;  $M_w = 300\,000$ ;  $M_n = 140\,000$ ) and poly(ethyl methacrylate) (PEMA;  $M_w = 340\,000$ ;  $M_n = 126\,000$ ) for the SHG studies were purchased from Scientific Polymer Products and used as received. Due to some photobleaching of the fluorescence probes in the as-received polymer, the polymers were washed several times by reprecipitation from dichloromethane/methanol before use in fluorescence measurements. The chromophore julolidenemalononitrile (JMN; Molecular Probes) was used as received. Disperse Red 1 (DR1; Aldrich) was recrystallized from toluene. The chromophore 4-(tricyanovinyl)-*N*-(2-hydroxyethyl)-*N*-ethylaniline (TC1) was synthesized according to a procedure by McKusick et al.<sup>32</sup> The random copolymer of isobutyl methacrylate and methacrylate monomer labeled with TC1 was synthesized using the procedure given in ref 30. The copolymer had a labeled monomer content of 0.5 mol % as determined by UV/visible absorbance. Figure 1 gives the structures of the polymers and chromophores used in this study.

The glass transition temperatures of all polymer systems were measured in a Perkin-Elmer DSC-7 differential scanning calorimeter using a 40 K/min cooling rate and 10 K/min heating rate.  $T_g$  was taken as the onset temperature of the heat capacity change. Table 1 lists all the polymer systems employed in this study and their corresponding  $T_g$ 's.<sup>33</sup>

**Sample Preparation.** Films for fluorescence measurements containing less than 0.005 wt % probe with respect to polymer were solvent cast from 7–10 wt % polymer solutions in spectrophotometric-grade dichloromethane (Aldrich) onto Q-grade quartz slides. These were allowed to dry overnight

**Table 1. Polymer–Chromophore System with Corresponding  $T_g$  and Fluorescence Quantum Yield,  $\Phi_f$** 

polymer	technique	chromophore	$T_g$ (°C)	$\Phi_f \times 10^2$
PiBMA	fluorescence	JMN <0.005 wt %	59	2.6
	SHG	JMN 2 wt %	53	
	fluorescence	TC1 < 0.005 wt %	59	0.37
	SHG	TC1 2 wt %	53	
PEMA	fluorescence	JMN <0.005 wt %	67	2.7
	SHG	JMN 2 wt %	61	
	fluorescence	TC1 < 0.005 wt %	67	0.75
	SHG	TC1 2 wt %	61	
iBMA–MATC1 (copolymer)	fluorescence	MATC1 0.5 mol %	64	4.8
	SHG	MATC1 0.5 mol %	64	

at room temperature and then for 3 days in a vacuum oven above  $T_g$  with resulting thicknesses on the order of 100  $\mu\text{m}$ . Samples for SHG measurements were made by dissolving 6–8 wt % polymer (and chromophore at 2 wt % relative to polymer for the doped systems) in spectroscopic-grade chloroform and spin coating onto a quartz substrate patterned with planar chrome electrodes (800  $\mu\text{m}$  gap) by standard photolithographic techniques. The films (2–5  $\mu\text{m}$  thick) were dried below  $T_g$  for 24 h and above  $T_g$  for 12 h under vacuum.

**Fluorescence Measurements.** Fluorescence spectra and quantum yields were obtained with a SPEX Fluorolog-2 DM1B fluorometer in front-face mode. Determination of the quantum yield of each chromophore was made at room temperature (298 K), immediately after quenching from above  $T_g$ , by referencing against perylene (Aldrich) in PMMA (with a quantum yield of 0.98<sup>34</sup>). The quantum yield for each system is listed in Table 1. The temperature dependence of the fluorescence behavior was obtained in the following manner. For  $T < T_g$ , after erasing thermal history by heating above  $T_g$ , the polymer film was quenched ( $\sim 5$  K/min) to a specified temperature, and the fluorescence intensity at maximum emission was monitored; excitation wavelengths,  $\lambda_{\text{ex}}$ , were 410 nm for JMN and 460 nm for TC1. At  $T > T_g$ , the samples were simply heated to the desired temperature, and the measurement was taken.

**SHG Measurements.** All SHG measurements were performed in decay mode and employed a Q-switched Nd–YAG laser (10 Hz frequency) with a 1.064  $\mu\text{m}$  fundamental beam. The measurement of reorientation dynamics from 20 s onward was done by monitoring the SHG intensity after switching off the dc-poling field permanently (15 kV/cm field). Rotational dynamics from 5  $\mu\text{s}$  to 2 s were monitored using a variable time delay for switching off the poling field with respect to the laser pulse. (See ref 6 for further details.) For studies done below  $T_g$ , the sample was heated above  $T_g$  and a dc-poling field was applied until steady state was reached in the rubbery state (poling time and temperature were chosen such that extraneous charge effects were negligible<sup>35</sup>); with the dc field applied, the sample was then quenched to the temperature of the decay measurement.

## Results and Discussion

**A. Second Harmonic Generation Studies.** A complete description of the basis for using SHG to quantify average rotational reorientation relaxation times of second-order nonlinear optical (NLO) chromophores doped in polymers is given in ref 6. A brief overview of the main features of this approach is provided below with the description of SHG data obtained for TC1 probes molecularly dispersed in PiBMA and PEMA and covalently attached to an iBMA-based copolymer. Comparisons to previous results<sup>6</sup> employing Disperse Red 1, which demonstrated strong coupling of its reorientation dynamics to the  $\alpha$ -relaxation dynamics of the polymers, will also be made.

In order to obtain SHG properties in an amorphous polymer containing intramolecular charge transfer chromophores, it is necessary to make the system noncentrosymmetric.<sup>36</sup> This requires applying a dc-poling field  $E_z$  near  $T_g$ , resulting in a net alignment of the NLO chromophores. For a steady-state situation (with con-

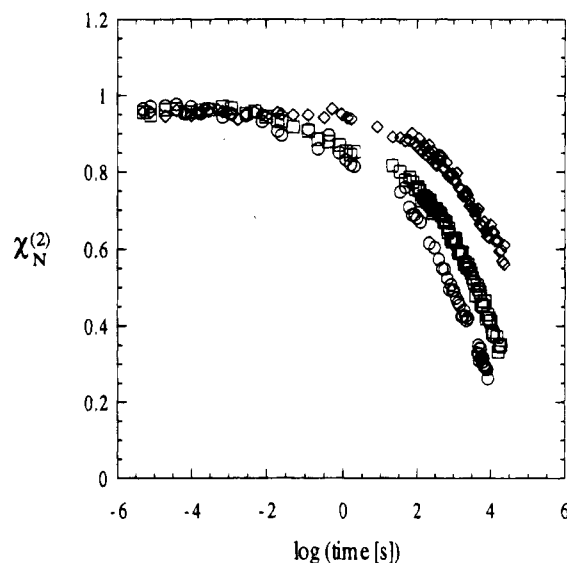


**Figure 2.** SHG decay mode measurements at 30 °C for (○) PiBMA + 2 wt % TC1, (□) PEMA + 2 wt % TC1, and (◇) iBMA–MATC1 copolymer.  $\chi_N^{(2)}$  is the value of  $\chi^{(2)}$  normalized with respect to its value just before turning off the dc-poling field.

tinuous application of the dc field), the SHG intensity,  $I(2\omega)$ , is given by<sup>37,38</sup>

$$[I(2\omega)]^{0.5} \propto \chi_{zzz}^{(2)} \propto NE_z^0 \left[ \frac{\mu\beta_{333}}{5kT} + \gamma \right] \quad (1)$$

where  $\chi_{zzz}^{(2)}$  is the second-order macroscopic susceptibility (hence abbreviated as  $\chi^{(2)}$ ),  $z$  is the direction of the incident polarization of the fundamental beam and the direction of the dc field, and  $N$  is the number density of the chromophores.  $\gamma$  is a contribution due to an electric field-induced third-order effect, which appears and disappears instantaneously upon application and removal of the dc field.<sup>37,39</sup> The term  $NE_z^0[\mu\beta/(5kT)]$ , where  $\mu$  is the dipole moment and  $\beta$  is the microscopic susceptibility of the NLO chromophore,  $k$  is the Boltzmann constant, and  $T$  is the absolute temperature, is due to the orientation of the chromophores which balances in response to the dc field and thermal randomization.

Figure 2 shows SHG decay mode measurements for several PiBMA- and PEMA-based systems relatively deep in the glassy state at 30 °C. The data are represented as  $\chi_N^{(2)}$ , which is  $\chi^{(2)}$  normalized to its value just prior to switching off the dc field. Within 5  $\mu\text{s}$  of the removal of the dc field,  $\chi_N^{(2)}$  has decreased to a value of 0.96 for all three systems represented, signifying a 4% decrease in  $\chi_N^{(2)}$  as compared to that before removal of the dc field. This 4% decrease is associated with the electric field-induced third-order effect for the TC1

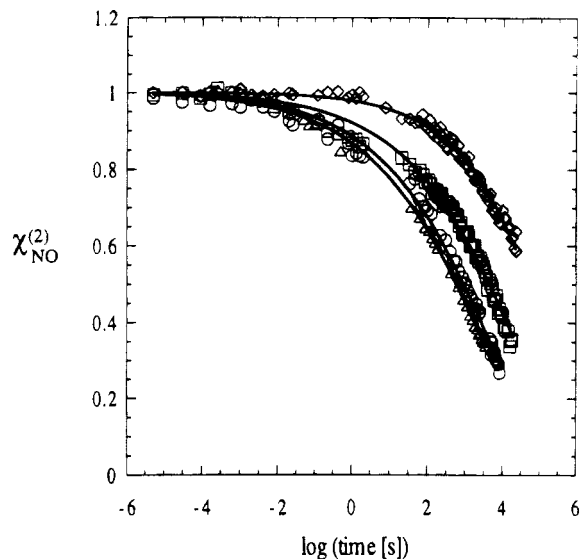


**Figure 3.** SHG decay data at 30 °C fitted to the KWW equation (solid lines) for (○) PiBMA + 2 wt % TC1, (□) PEMA + 2 wt % TC1, and (◇) iBMA-MATC1 copolymer. Included as a comparison is the decay for (△) PiBMA + 2 wt % DR1 at the same temperature.  $\chi_{\text{NO}}^{(2)}$  corresponds to the orientational component of  $\chi^{(2)}$ .

probe. (Similar measurements for a variety of NLO probes have demonstrated that the relative electric field-induced third-order contribution to the steady-state  $\chi^{(2)}$  value can range from several percent to 20% or higher depending on the chromophore<sup>37,40</sup>.)

Figure 3 shows the decay-mode dynamics at 30 °C associated only with the orientational component of  $\chi_N^{(2)}$ , here designated  $\chi_{\text{NO}}^{(2)}$ , for TC1 and Disperse Red 1 doped at 2 wt % in PiBMA, for TC1 doped at 2 wt % in PEMA, and for the iBMA-based copolymer containing 0.5 mol % TC1.  $\chi_{\text{NO}}^{(2)}$  has been calculated for a given decay time using eq 2, where  $y$  represents the fraction

$$\chi_{\text{NO}}^{(2)}(t) = \frac{X_N^{(2)}(t)}{(1-y)} \quad (2)$$

of the steady-state  $\chi^{(2)}$  associated with the instantaneous electric field-induced effect.<sup>37</sup> As indicated above,  $y = 0.04$  for TC1 probe and label while a previous study determined  $y = 0.12$  for Disperse Red 1 in methacrylate-based polymers at a doping concentration of 2 wt %. Noteworthy is the substantial breadth of the relaxation times in all cases with the data for the 2 wt % TC1 and Disperse Red 1 in PiBMA nearly overlapping. This suggests that the reorientation dynamics of these two probes are coupled in the same way to polymer dynamics. As the glass transition temperature is higher in PEMA than in PiBMA, there is a substantial increase in the temporal stability of  $\chi^{(2)}$  measured at a given temperature for PEMA relative to PiBMA. A similar  $T_g$  effect is observed in the iBMA-based copolymer sample containing 0.5 mol % TC1 (which has a substantially higher  $T_g$  than the doped PiBMA samples due to the different local tacticity resulting from the polymerization conditions used in preparing the copolymer and slight plasticization effects due to the TC1 chromophore dopant). Beyond this effect, we also note that the copolymer sample has a substantially longer plateau region at short times for  $\chi_{\text{NO}}^{(2)}$  than any of the doped cases. Such behavior has been noted before<sup>30</sup> in iBMA-based copolymers containing covalently attached Dis-

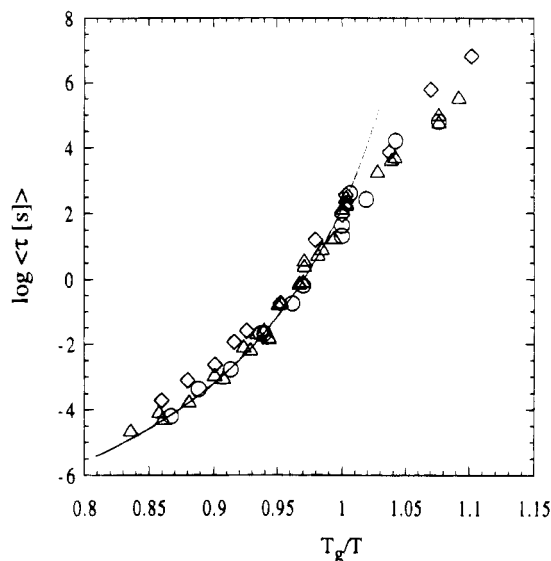


**Figure 4.** Values of  $\langle \tau \rangle$  obtained from SHG measurements scaled using the reduced variable  $T_g/T$ : (○) PiBMA + 2 wt % TC1; (□) PEMA + 2 wt % TC1; (◇) iBMA-MATC1 copolymer; (△) PiBMA + 2 wt % DR1. The solid curve corresponds to the PiBMA + 2 wt % DR1 data at  $T \geq T_g$  fitted to the WLF equation resulting in values of  $C_1 = 12$  K and  $C_2 = 45$  K.

perse Red 1 chromophores; this has been attributed to the additional degree of freedom for the free probe as compared with the side-chain functionalized system where motion is slightly constrained by covalent attachment. Consequently, even at equivalent temperatures relative to  $T_g$ , a small yet measurable additional degree of reorientation can occur at shorter times in the free probe system indicative of a broader distribution of relaxation times.

The solid curves in Figure 3 correspond to fits using the Kohlrausch-Williams-Watts (KWW) equation<sup>41</sup>

$$\chi_{\text{NO}}^{(2)} = \exp[-(t/\tau)^{\beta_w}] \quad (3)$$

where  $\tau$  and  $\beta_w$  are the KWW parameters.  $\beta_w$  can take values between 0 and 1;  $\beta_w = 1$  corresponds to a single-exponential decay (single relaxation time) while  $\beta_w < 1$  indicates a distribution of relaxation times. If a SHG polymeric system exhibits a relaxation of the orientation component of  $\chi^{(2)}$  which may be fit adequately to eq 3 at a variety of temperatures, then a comparison of polymer dynamics to the decay of  $\chi^{(2)}$  may be achieved by defining an average rotational, reorientation relaxation time constant,  $\langle \tau \rangle$ :

$$\langle \tau \rangle = \int_0^\infty \exp\left[-\left(\frac{t}{\tau}\right)^{\beta_w}\right] dt = \frac{\tau \Gamma(1/\beta_w)}{\beta_w} \quad (4)$$

where  $\Gamma$  is the gamma function. This definition of  $\langle \tau \rangle$  is similar to that used in studies of low molecular weight glass-former and polymer dynamics by various techniques.<sup>23,42,43</sup>

Figure 4 compares  $\langle \tau \rangle$  values for the TC1 and Disperse Red 1 doped and copolymer systems. Data have been scaled with the reduced variable  $T_g/T$ . This scaling technique has been used by Angell<sup>28</sup> to compare the macroscopic viscosity of glass-forming materials and by Roland and Ngai<sup>44</sup> to compare  $\alpha$ -relaxation dynamics of various linear polymers. It has also been used previously in SHG studies to demonstrate that relative to  $T_g$  the temperature dependence of the rotational reorientation dynamics of Disperse Red 1 are identical

in PiBMA and PEMA but different in polystyrene above  $T_g$ .<sup>7</sup> Several important points are evident from the excellent overlap of data in Figure 4. First, relative to  $T_g$  the temperature dependence of the reorientation dynamics of a TC1 dopant is similar in PiBMA and PEMA. Second, the reorientation dynamics of Disperse Red 1 and TC1 are also similar in PiBMA. Finally, relative to  $T_g$ , the average reorientation relaxation time is only slightly affected by covalent attachment of Disperse Red 1 and TC1 to PiBMA. It is important to add that covalent attachment of the probe to the polymer backbone narrows the distribution of the relaxation spectrum by removing the shorter time components. However, because the short time contributions are small compared to the overall distribution,  $\langle\tau\rangle$  is altered relatively little.<sup>45</sup> Given that previous work<sup>6</sup> has established the strong coupling of the reorientation dynamics of Disperse Red 1 to the  $\alpha$ -relaxation dynamics of PiBMA and PEMA, the same conclusion must be drawn for the TC1 probe in PiBMA (free probe and attached) and in PEMA.

The relationship between the polymer  $\alpha$ -relaxation dynamics and the TC1 probe reorientation dynamics is further reinforced by the excellent fit of the rubbery-state PiBMA and PEMA data to the WLF equation<sup>27</sup>:

$$\log\left(\frac{\langle\tau\rangle}{\langle\tau\rangle_{T_g}}\right) = \frac{-C_1(T - T_g)}{C_2 + T - T_g} \quad (5)$$

with  $C_1 = 11$  K and  $C_2 = 49$  K for PiBMA and nearly identical values being obtained ( $C_1 = 13$  K and  $C_2 = 51$  K) for PEMA, in reasonably good agreement with literature values of the WLF parameters for methacrylate-based polymers.<sup>24,43,46</sup> (Similar values were obtained for Disperse Red 1 in PiBMA and PEMA. See Table 2.) The facts that  $\langle\tau\rangle$  is  $\sim 100$  s at  $T_g$  and that below  $T_g$  the reorientation dynamics exhibit a weaker temperature dependence (which can be described by an apparent Arrhenius-type behavior over the limited temperatures below  $T_g$ ) are also signatures of  $\alpha$ -relaxation dynamics in amorphous polymers and low molecular weight glass formers.<sup>28,44</sup>

It is noteworthy that besides excellent agreement in  $\langle\tau\rangle$  values, doped TC1 and Disperse Red 1 probes exhibit excellent agreement in  $\beta_w$  values determined from plots such as those in Figure 3. Below  $T_g$ ,  $\beta_w$  is  $\sim 0.25$  and independent of temperature (for the limited temperature range tested) for both probes. Above  $T_g$ ,  $\beta_w$  increases with increasing temperature, with values of  $\sim 0.40$  being achieved at 20 °C above  $T_g$ , indicating that at temperatures slightly above  $T_g$  the  $\alpha$ -relaxation dynamics of these polymers do not exhibit thermorheological simplicity; i.e., the breadth of the distribution of  $\alpha$ -relaxation times is not temperature independent. This similarity in reorientation relaxation features of the two probes illustrates that if the probe reorientation is fully coupled to the polymer  $\alpha$ -relaxation (due to the significant size of the probe), then moderate differences in size or shape of the probe (as in TC1 or Disperse Red 1) may not significantly alter  $\langle\tau\rangle$  or the distribution of reorientation relaxation times of the probe. (However, when the probe becomes sufficiently small, even rather subtle changes in probe structure can result in at least a partial decoupling of its reorientation dynamics from the polymer cooperative segmental dynamics associated with the  $\alpha$ -relaxation, with major changes in  $\langle\tau\rangle$  and  $\beta_w$  being evident with even small changes in probe size or shape. Examples of such effects<sup>40</sup> will be described fully

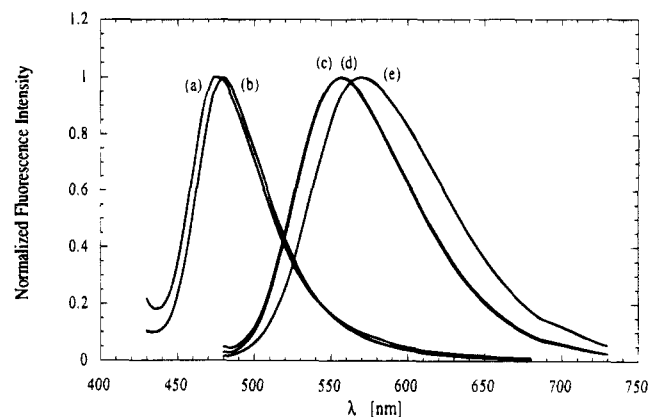


**Figure 5.** Normalized fluorescence emission spectra for JMN in (a) PiBMA and (b) PEMA excited at 410 nm and for TC1 in (c) PiBMA, (d) PEMA, and (e) iBMA-MATC1 copolymer excited at 460 nm.

in the near future.<sup>47</sup> Additionally, very large SHG probes may show a narrower distribution of relaxation times than TC1 or Disperse Red 1 in polymers near  $T_g$ .<sup>48)</sup>

**B. Fluorescence Studies.** In section A it was established by SHG measurements that the rotational reorientation dynamics of the TC1 probe are strongly coupled to the polymer  $\alpha$ -relaxation dynamics in rubbery and glassy PiBMA and PEMA near  $T_g$ . It now becomes important to determine the validity of Loutfy's suggestion<sup>18</sup> that the temperature dependence of the rotational (and/or isomerization) motions (illustrated in Figure 1) associated with the nonradiative decay pathway from the excited state of the rotor probes may be described by the WLF equation, implying that they are also coupled to the  $\alpha$ -relaxation dynamics.

In order to test fully this suggestion, two rotor probes molecularly dispersed in polymer were studied. As Loutfy used dicyanovinyl-based rotor probes exclusively,<sup>18,19</sup> the probe JMN (see Figure 1) was tested. In order to draw comparisons with SHG studies described in section A, the tricyanovinyl-based probe TC1 was studied, both molecularly dispersed in and covalently attached to the polymer. Figure 5 illustrates the fluorescence spectra of the rotor probes JMN and TC1 molecularly dispersed in PiBMA and of the TC1 chromophore covalently attached to the iBMA-based copolymer. The factor of 13 increase in quantum yield,  $\Phi_f$ , upon attachment of TC1 to the polymer (see Table 1 for quantum yields at 25 °C) may be attributed to the fact that the dialkylamino-based electron-donor group loses mobility upon attachment to the polymer, resulting in a significant reduction in the contribution to the "rotor" nature of the probe and, therefore, an increase in quantum yield. This explanation is further supported by the fact that the JMN probe, which has the smaller dicyanovinyl electron-acceptor moiety in place of the tricyanovinyl moiety found in TC1, also has a higher  $\Phi_f$  than doped TC1. (If the only difference in structure were the dicyanovinyl and tricyanovinyl groups, the dicyanovinyl-based probe would have a lower  $\Phi_f$  based on the smaller size and therefore lower resistance to rotation during the excited-state lifetime of the probe.<sup>49,50</sup>) The higher  $\Phi_f$  in JMN is due to the total immobilization of its electron-donor moiety by covalent linkage to the aromatic ring. (See Figure 1 for a comparison of TC1 and JMN structures.)

The temperature dependence of probe fluorescence spectra can be used to determine the temperature

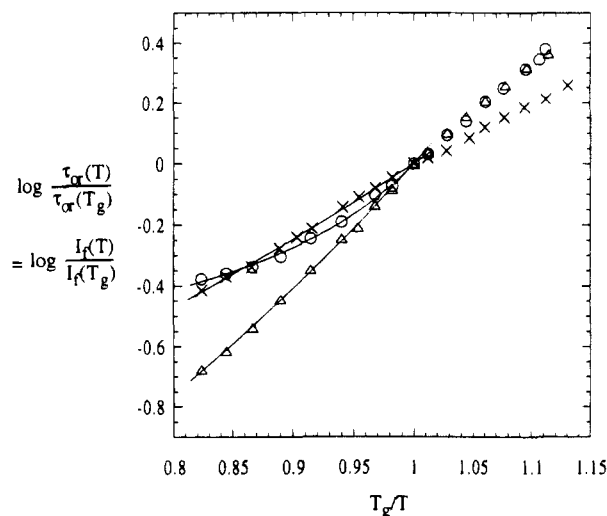


**Figure 6.** Temperature dependence of the fluorescence intensity normalized with respect to the fluorescence intensity at  $T_g$  as a function of the reduced variable  $T_g/T$  for ( $\Delta$ ) JMN in PiBMA, ( $\circ$ ) TC1 in PiBMA, and ( $\times$ ) iBMA-MATC1 copolymer. Curves correspond to fits to eq 5 at  $T \geq T_g$ ; for parameters, see Table 2.

dependence of the orientational relaxation time,  $\tau_{or}$ , for the internal (nonradiative decay-related) rotation of the rotor on the probe. In particular,  $\tau_{or}$  can be related to  $\Phi_f$  by<sup>18</sup>

$$\tau_{or} = \tau_r \left( \frac{\Phi_f}{\Phi_0 - \Phi_f} \right) \quad (6)$$

where  $\Phi_0$  is the limiting fluorescence quantum yield at minimum free volume, which Loutfy and Arnold<sup>18b</sup> indicated may be taken as 1, and  $\tau_r$  is the intrinsic radiative lifetime of the excited state. From eq 6 and the fact that  $I_f(T)/I_f(T_{ref}) = \Phi_f(T)/\Phi_f(T_{ref})$ , the relative temperature dependence of  $\tau_{or}$  can be determined using measures of the fluorescence intensity and quantum yield:

$$\frac{\tau_{or}(T)}{\tau_{or}(T_{ref})} = \frac{I_f(T)}{I_f(T_{ref})} \left[ \frac{1 - \Phi_f(T_{ref})}{1 - \Phi_f(T)} \right] \quad (7)$$

where  $I_f$  represents the fluorescence intensity at a given wavelength. (For an extremely small  $\Phi_f$ , as is the case for the systems studied here, eq 7 reduces to  $I_f(T)/I_f(T_{ref})$ .) The ability to measure this relative temperature dependence with steady-state fluorescence intensities instead of excited-state lifetimes is important as the lifetimes of the rotor probes are often very short<sup>18b</sup> and difficult to measure accurately with conventional fluorescence decay measurements, where available, for lifetime characterization.

The relative temperature dependencies of  $\tau_{or}$  for JMN and TC1 (probe and covalently attached) in PiBMA and PEMA are given in Figures 6 and 7. (These data are plotted in a format similar to that used in Figure 4 for  $\langle \tau \rangle$  values determined from SHG measurements). One noteworthy feature of the data is the substantially smaller temperature dependence of the  $\tau_{or}$  data for the JMN probe relative to the TC1 probe. That different rotor probes provide different sensitivity as a function of temperature may be expected from Loutfy's picture of the probe sensitivity to free volume in the polymer.<sup>51</sup> Loutfy<sup>18</sup> indicated that the rotation-dependent nonradiative decay rate,  $k_{nr}$ , is related to the medium free-

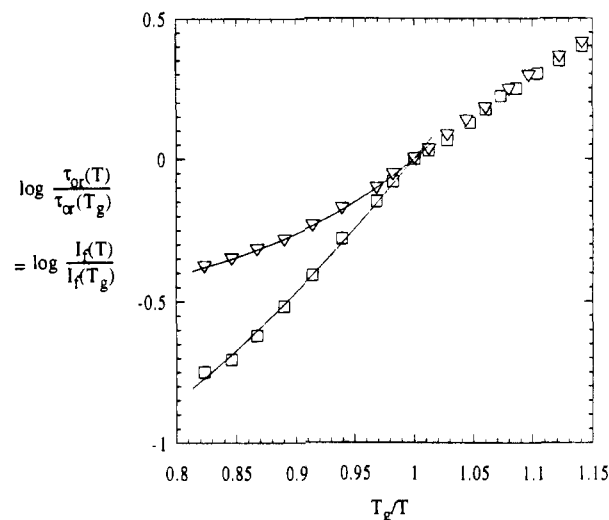


**Figure 7.** Temperature dependence of the fluorescence intensity normalized with respect to fluorescence intensity at  $T_g$  as a function of the reduced variable  $T_g/T$  for ( $\nabla$ ) JMN in PEMA and ( $\square$ ) TC1 in PEMA. Curves correspond to fits to eq 5 at  $T > T_g$ ; for parameters, see Table 2.

volume fraction,  $f$ , and the occupied volume fraction,  $f_0$ , according to

$$k_{nr} = k_{nr}^0 \exp(-xf_0/f) \quad (8)$$

where  $k_{nr}^0$  is the free rotor reorientation rate (essentially that would be found in a vacuum and independent of temperature). Furthermore, Loutfy stated that "x is a constant for the particular probe".<sup>18b</sup> The nonradiative decay rate is related to fluorescence quantum yield by

$$\Phi_f = \frac{k_r}{k_r + k_{nr}} \quad (9)$$

where  $k_r$  is the radiative decay rate (also independent of temperature<sup>52</sup>). Combining eqs 8 and 9 yields

$$\frac{\Phi_f}{1 - \Phi_f} = \frac{k_f}{k_{nr}^0} \exp\left(\frac{xf_0}{f}\right) \quad (10)$$

In the limit of small  $\Phi_f$ , this reduces to

$$\Phi_f = \frac{k_r}{k_{nr}^0} \exp\left(\frac{xf_0}{f}\right) \quad (11)$$

This is analogous in form to Doolittle's expression<sup>53</sup> relating the temperature dependence of the viscosity of paraffinic molecules to free volume, the temperature dependence of which is related to thermal expansion. (The WLF equation may be derived using Doolittle's expression as a starting point.<sup>27,46</sup>)

A second noteworthy feature of the data in Figures 6 and 7 is the much smaller temperature dependence, especially above  $T_g$ , of the fluorescence-related orientational relaxation time,  $\tau_{or}$ , as compared with that of the SHG-related average reorientation relaxation time,  $\langle \tau \rangle$ , given in Figure 4. This difference is made clear in Figure 8 by comparing the relative temperature dependence of  $\tau_{or}$  and  $\langle \tau \rangle$  for TC1. While the  $\tau_{or}$  data above  $T_g$  in Figures 6 and 7 may be fit to a WLF-type equation for all chromophore/polymer systems studied here, the values of the WLF parameters obtained from such fits

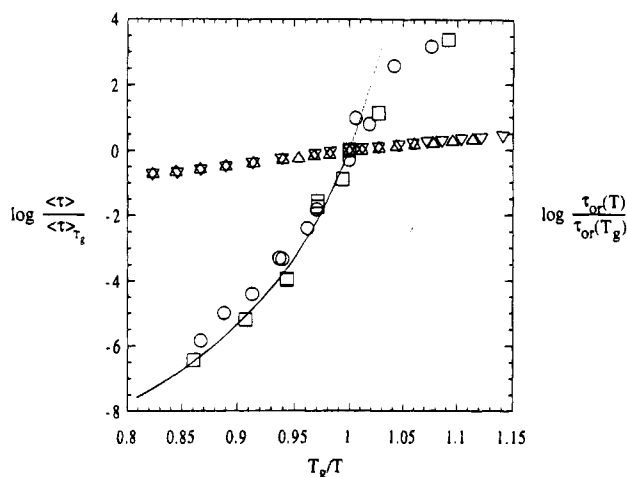


**Figure 8.** Relative reorientational relaxation times associated with the different motions of TC1 observed in SHG measurements for (○) PiBMA and (□) PEMA as compared to fluorescence measurements for (△) PiBMA and (▽) PEMA.

are far outside the range expected for systems exhibiting behavior coupled to the polymer  $\alpha$ -relaxation. Table 2 compares values of  $C_1$  and  $C_2$  obtained from fitting eq 5 to SHG and fluorescence data for  $T > T_g$  given in Figures 4, 6, and 7 as well as from the research literature for neat PEMA. (Typical WLF parameters describing the temperature dependence of  $\alpha$ -relaxation processes in simple, linear, carbon backbone polymers range from approximately 10 to 20 K for  $C_1$  and 40 to 100 K for  $C_2$  when  $T_g$  is used as the reference temperature.<sup>46</sup>) In particular, the exceedingly small values of the  $C_1$  parameters obtained in all the fluorescence experiments, roughly 5–20% of the values obtained either from the SHG measurements or from the literature for the  $\alpha$ -relaxation process in PEMA,<sup>24</sup> effectively preclude substantial coupling of the nonradiative decay rotational motions of the fluorescence probes to the  $\alpha$ -relaxation process. (It should be noted that a slightly different temperature dependence is observed for the labeled TC1 system as compared to the free TC1 case.)

While it is clear from the available data that the nonradiative rotational decay processes for TC1 and JMN are not fully coupled to the  $\alpha$ -relaxation in PEMA and PiBMA, there are several possible interpretations available for explaining the temperature dependence of  $\tau_{or}$ . One approach considers that only a fraction of the chromophores exhibits coupling to the  $\alpha$ -relaxation process, with that fraction represented by the parameter  $x$  in eq 10 or by another parameter  $\xi$  (employed in an earlier study by Ehlich and Sillescu,<sup>24</sup> who investigated the coupling of the translational diffusion of probes to polymer relaxation), related directly to  $x$ . A value of  $x = 1$  may be interpreted as indicating complete coupling of the probe motions to the  $\alpha$ -relaxation processes in the polymer while a value of  $x = 0$  may be interpreted as indicating no coupling.

Assuming the validity of eq 10,  $\tau_{or}(T)$  may be given by

$$\frac{\tau_{or}(T)}{\tau_{or}(T_{ref})} = \exp \left\{ x \left[ \frac{1}{f(T)} - \frac{1}{f(T_{ref})} \right] \right\} \quad (12)$$

Over a limited temperature range in the rubbery state, the free volume fraction in a polymer (assumed sensitive to  $\alpha$ -relaxation processes) varies linearly with temper-

ature according to

$$f = f_g + \alpha_f(T - T_g) \quad (13)$$

where  $f_g$  is the fractional free volume at  $T_g$  and  $\alpha_f$  is the difference in thermal expansion coefficients above and below  $T_g$ . From the research literature,<sup>24</sup>  $f_g = 0.028$  and  $\alpha_f = 3.1 \times 10^{-4} \text{ K}^{-1}$  for PEMA. Similar data were not available for PiBMA; for simplicity, it was assumed that  $f_g$  and  $\alpha_f$  were identical to those for PEMA. Using these values in combination with eqs 12 and 13, the data in Figures 6 and 7 were fit to yield values of  $x$ , listed in Table 2. (This type of analysis was also performed by Loutfy and Arnold<sup>18b</sup> on fluorescence data for JMN in highly viscous liquids in a study in which  $x$  was determined by freely fitting the temperature data to an expression similar to eq 12.)

The values of  $x$  ranging from 0.056 to 0.11, depending on the probe/polymer system, suggest that at most there is little coupling of the probe nonradiative decay motions to the  $\alpha$ -relaxation process. The smaller values of  $x$  for the JMN probe as compared to the TC1 probe in both PiBMA and PEMA may be related to the additional rotational motion of the dialkylamino group in the TC1 probe as well as the fact that rotation of the electron-acceptor moiety on TC1 involves three cyano groups instead of only two cyano groups as in JMN. The motion of larger moieties may be expected to exhibit greater coupling to the cooperative segmental relaxations in polymers such as the  $\alpha$ -relaxation process. In addition, the smaller values of  $x$  in the iBMA-MATC1 system as compared to the free TC1 probe in PiBMA may be attributed to the covalent attachment of the dialkylamino group to the polymer backbone, creating hindrance to rotation analogous to the complete "tying down" of the amino group in JMN. As is evident, the temperature dependence of the fluorescence of the free JMN and covalently attached TC1 nearly overlap.

Ehlich and Sillescu<sup>24</sup> analyzed the extent of coupling of the probe translational diffusion to the cooperative polymer segmental motions associated with the  $\alpha$ -relaxation process using a coupling parameter,  $\xi$ , where  $0 \leq \xi \leq 1$ , with a value of 0 signifying no coupling and a value of 1 corresponding to complete coupling. Rather than allowing the WLF parameters  $C_1$  and  $C_2$  to be freely fitted to the experimental diffusion data, they used values of  $C_1$  and  $C_2$  representative of the polymer the  $\alpha$ -relaxation dynamics (taken from dynamic mechanical analysis) and fit the data to the modified WLF equation below:

$$\log \left( \frac{D(T_g)}{D(T)} \right) = \frac{-\xi C_1(T - T_g)}{C_2 + T - T_g}, \quad T \geq T_g \quad (14)$$

where  $D$  is the probe translational diffusion coefficient. Here, the same approach is used except the temperature dependence is analyzed in terms of  $\tau_{or}$ :

$$\log \left( \frac{\tau_{or}(T)}{\tau_{or}(T_g)} \right) = \frac{-\xi C_1(T - T_g)}{C_2 + T - T_g}, \quad T \geq T_g \quad (15)$$

By fitting the data in Figures 6 and 7 to eq 15 and using  $C_1 = 15 \text{ K}$  and  $C_2 = 90 \text{ K}$ ,<sup>24</sup> values of  $\xi$  were determined to be small for all polymer systems, ranging from 0.058 to 0.11.<sup>54</sup> (See Table 2.) These very small values also suggest that at most there is little coupling of the rotational motions of rotor probe donor and/or acceptor groups to the polymer  $\alpha$ -relaxation. (In con-



Table 2. WLF Parameters and Values of  $x$ ,  $\xi$ , and Apparent Activation Energy,  $E_a$ <sup>a</sup>

polymer	technique	probe	$C_1$	$C_2$ (K)	$x$	$\xi$	$E_a$ (kcal/mol)
PiBMA	fluorescence	JMN	0.68	53	0.059	0.061	3.3
PiBMA	fluorescence	TC1	2.4	176	0.095	0.098	5.8
PEMA	fluorescence	JMN	0.75	68	0.056	0.058	3.3
PEMA	fluorescence	TC1	2.5	165	0.11	0.11	6.9
iBMA-MATC1 <sup>b</sup>	fluorescence	TC1 <sup>b</sup>	1.6	207	0.057	0.059	3.7
PiBMA	SHG	TC1	11	48			
PEMA	SHG	TC1	13	51			
iBMA-MATC1 <sup>b</sup>	SHG	TC1 <sup>b</sup>	12	53			
PiBMA	SHG <sup>40</sup>	DR1	12	45			
PEMA	SHG <sup>40</sup>	DR1	13	51			
PEMA <sup>c</sup>	DMA <sup>46</sup>		17.6	65.5			
PEMA <sup>c</sup>	DMA <sup>24</sup>		15	90			

<sup>a</sup>  $C_1$  and  $C_2$  parameters were obtained from fitting fluorescence data to the WLF equation ( $T \geq T_g$ ) with respect to a reference temperature at  $T_g$ . Values for  $x$  and  $\xi$  were determined by fitting fluorescence data to eqs 12 and 15. Included as a comparison are  $C_1$  and  $C_2$  for the same polymers as determined by second harmonic generation (SHG) measurements using the Disperse Red 1 probe and dynamic mechanical analysis (DMA), where available.  $E_a$  was determined from an Arrhenius fit for  $T > T_g$ . <sup>b</sup> TC1 covalently attached. <sup>c</sup> Neat PEMA.

trast, for the probe translational diffusion studied by Ehlich and Sillescu, typical values of  $\xi$  ranged from 0.50 to 0.84, depending on the probe and polymer, suggesting not necessarily complete but certainly substantial coupling of translational motion to the polymer  $\alpha$ -relaxation.<sup>24)</sup>

As with the interpretation based on  $x$  values, the  $\xi$  values determined from eq 15 are clearly larger for TC1 than JMN, presumably due to the larger size of the nonradiative decay motions in the former. Similar to the interpretation based on the  $x$  values, the TC1-labeled copolymer yielded  $\xi$  values nearly identical to those of JMN rather than the free probe TC1, presumably due to the very similar temperature dependence of the fluorescence of JMN and the covalently attached TC1. Furthermore, the similar values of  $\xi$  as compared to  $x$  using eqs 12 and 15 suggest that both methods are equivalent. This can be easily shown by recalling Doolittle's expression for viscosity,  $\eta$ , in terms of free volume:<sup>53</sup>

$$\eta = A \exp(-Bf_0/f) \quad (16)$$

where  $A$  and  $B$  are constants. A comparison of eqs 11, 12, 15, and 16 reveals that  $x = \xi B$ , and  $B$  is usually assigned a value of 1.<sup>46</sup> Hence, Loutfy's probe-dependent parameter,  $x$ , can be similarly viewed as a coupling parameter.

We note that the ability to fit experimental probe or label relaxation data to a WLF equation, or equivalently a Vogel-Tamman-Fulcher equation, without regard to the values of the parameters determined from the fit, has sometimes been misinterpreted<sup>55</sup> in the SHG literature as indicating coupling to the cooperative segmental motions associated with the polymer  $\alpha$ -relaxation. Reports of success modeling SHG data by the WLF equation with anomalous  $C_1$  and  $C_2$  values, such as  $C_1 = 2.35$  K and  $C_2 = 17.02$  K (for  $T_{\text{ref}} = T_g$ ) cited in ref 55, instead indicate that, based on interpretations employing either  $x$  or  $\xi$  values, at most there is little coupling of SHG dynamics to the polymer  $\alpha$ -relaxation. It should also be noted that over a small enough temperature range ( $\leq 30$  °C) a purely Arrhenius set of data may be fit with reasonable statistics to a WLF-type equation. Consequently, merely fitting relaxation data to a WLF-type equation is not sufficient to claim substantial coupling to polymer  $\alpha$ -relaxation dynamics. Instead, other characteristics, including the values of the WLF parameters obtained from such a fit, the time scales associated with the relaxation, and the change to a weaker temperature dependence below  $T_g$  (assum-

ing absence of or negligible physical aging in the sample near  $T_g$ ) must also be carefully considered before drawing conclusions about coupling to cooperative segmental motion in polymers.

A final possible interpretation of the  $x$  and  $\xi$  values listed in Table 2 is that the nonradiative decay rotations of moieties on the probes are related to sub- $\alpha$ -relaxations, which may include  $\beta$ -relaxations (in PEMA this has been interpreted as involving a 180° flip of the carboxyl group coupled to a rocking motion of the local chain axis<sup>56)</sup> as well as smaller scale  $\gamma$ -relaxations. In the discussion above regarding determination of  $x$  or  $\xi$  values, the coupling of probe motions to polymer relaxations was considered without regard to the time scales involved in the nonradiative decay motions of the probes. The nonradiative lifetime, or the time required for the charge transfer acceptor and/or donor to rotate on the chromophore, is on the order of nanoseconds<sup>18,48</sup> for both JMN and TC1. The fact that at  $T_g$  the average time scales of the cooperative segmental motions in PiBMA and PEMA are on the order of 100 s argues against the coupling of the probe motions to the  $\alpha$ -relaxation.

In the case of the  $\beta$ -relaxation in PEMA, the characteristic relaxation time near  $T_g$  is on the order of milliseconds<sup>56,57</sup> with an apparent activation energy of  $\sim 20$  kcal/mol near  $T_g$ . Although no characteristic relaxation times were found in the research literature for  $\gamma$ -relaxations in PiBMA or PEMA, for other poly(alkyl methacrylates) such as methyl, *n*-propyl, and *n*-butyl, time scales of the  $\gamma$ -relaxation near  $T_g$  are several orders of magnitude faster than those of the  $\beta$ -relaxation.<sup>58,59</sup> Given that the nonradiative rotational motion of moieties on the rotor probes occurs on the time scales of nanoseconds, and the apparent activation energies for free or labeled chromophore fluorescence (see Figures 6 and 7) are approximately 3–7 kcal/mol<sup>60</sup> for  $T \geq T_g$ , it appears that exclusive coupling of the rotor probe motion to the  $\beta$ -relaxation is ruled out as well. Instead, it is likely that the nonradiative rotational motions of the probe molecules are coupled to at most a combination of  $\gamma$ - and  $\beta$ -relaxations and that free rotation, independent of any coupling to the polymer matrix, may be present for a fraction of the chromophores. Further studies, especially with regard to the temperature dependence of the fluorescence lifetimes in these systems, will be needed to provide definite descriptions of coupling between the probe and polymer dynamics.



## Conclusions

The rotational reorientation of the molecular probe TC1 characterized by SHG is substantially coupled to the  $\alpha$ -relaxation in PiBMA and PEMA. This is apparent from the values of the average rotational reorientation relaxation time,  $\langle\tau\rangle$ , at  $T_g$ , the weaker temperature dependence of  $\langle\tau\rangle$  below  $T_g$  as compared to above  $T_g$ , and the nearly identical temperature dependence of  $\langle\tau\rangle$  for TC1 and Disperse Red 1, the latter probe having been previously shown<sup>6</sup> to have its SHG reorientation dynamics coupled to the  $\alpha$ -relaxation in these polymers. In contrast, using the approaches employed previously by Loutfy<sup>18</sup> and Ehlich and Sillescu<sup>24</sup> for analyzing the temperature dependence of probe dynamics, the rotor motions of TC1 and JMN, as characterized by fluorescence measurements, were shown to be largely decoupled from the polymer  $\alpha$ -relaxation. Furthermore, fluorescence time scales and apparent activation energy arguments suggest that the rotor motions may be substantially associated with sub- $\beta$ -relaxation processes. Consequently, while the WLF equation, describing the rubbery-state temperature dependence of cooperative segmental motions in polymers, is an appropriate means of modeling the temperature dependence of rotational reorientation of sufficiently large probes such as TC1, it is inappropriate for describing the rotor motions of such probes studied by fluorescence which are, at a minimum, very significantly decoupled from  $\alpha$ -relaxations.

While SHG and fluorescence measurements involving rotor probes provide sensitivity to distinct issues concerning polymer relaxation dynamics, they may both prove useful in discerning differences in relaxation behavior in thin versus ultrathin polymer films. In such studies, optical approaches may be expected to have a significant advantage over methods such as mechanical property characterization or differential scanning calorimetry. Such effects of film thickness on physical aging rates and apparent glass transition measurements have recently been studied via fluorescence;<sup>61,62</sup> SHG investigations will also be undertaken in order to draw conclusions about changes in  $\alpha$ -relaxation dynamics as film thicknesses approach several polymer radii of gyration.

**Acknowledgment.** We gratefully acknowledge the support provided by the National Science Foundation through the MRL program of the Materials Research Center of Northwestern University, under Award DMR-9120521. We also acknowledge our helpful interactions with Professor George K. Wong (Physics and Astronomy Department, Northwestern University).

## References and Notes

- Kluin, J. E.; Moaddel, H.; Ruan, M. Y.; Yu, Z.; Jamieson, A. M.; Simha, R.; McGervey, J. D. *Adv. Chem.* **1993**, 236, 535.
- Ediger, M. D. *Annu. Rev. Phys. Chem.* **1991**, 42, 225.
- Davies, M.; Edwards, A. *Trans. Faraday Soc.* **1967**, 63, 2163.
- Hains, P. J.; Williams, G. *Polymer* **1975**, 16, 725.
- (a) Mansour, A. A.; Stoll, B. *Colloid Polym. Sci.* **1992**, 270, 219. (b) *Ibid.* **1994**, 272, 17. (c) *Ibid.* **1994**, 272, 25.
- Dhinojwala, A.; Wong, G. K.; Torkelson, J. M. *Macromolecules* **1993**, 26, 5943.
- Dhinojwala, A.; Wong, G. K.; Torkelson, J. M. *J. Chem. Phys.* **1994**, 100, 6046.
- Tsay, F.-D.; Gupta, A. *J. Polym. Sci., Polym. Phys. Ed.* **1987**, 25, 855.
- Shimada, S. *Prog. Polym. Sci.* **1992**, 17, 1045.
- (a) Rössler, E.; Taupitz, K.; Börner, K.; Schulz, M.; Vieth, H.-M. *J. Chem. Phys.* **1990**, 92, 5847. (b) Rössler, E.; Börner, K.; Schulz, M.; Taupitz, K. *J. Non-Cryst. Solids* **1991**, 131–133, 99.
- (a) Lamarre, L.; Sung, C. S. P. *Macromolecules* **1983**, 16, 1729. (b) Yu, W. C.; Sung, C. S. P.; Robertson, R. E. *Macromolecules* **1988**, 21, 355.
- (a) Victor, J. G.; Torkelson, J. M. *Macromolecules* **1987**, 20, 2241. (b) *Ibid.* **1987**, 20, 2951; (c) *Ibid.* **1988**, 21, 3490. (d) Royal, J. S.; Victor, J. G.; Torkelson, J. M. *Macromolecules* **1992**, 25, 729. (e) Royal, J. S.; Torkelson, J. M. *Macromolecules* **1992**, 25, 4792.
- (a) Kanato, H.; Tran-Cong, Q.; Hua, D. H. *Macromolecules* **1994**, 27, 7907. (b) Tran-Cong, Q.; Chikaki, S.; Kanato, H. *Polymer* **1994**, 35, 4465.
- (a) Royal, J. S.; Torkelson, J. M. *Macromolecules* **1990**, 23, 3536. (b) *Ibid.* **1992**, 25, 1705. (c) *Ibid.* **1993**, 26, 5331.
- (a) Bokobza, L.; Pham-van-Cang, C.; Giordana, C.; Monnerie, L.; Vandendriessche, J.; De Schryver, F. C.; Kontos, E. G. *Polymer* **1987**, 28, 1876. (b) Bokobza, L.; Pham-van-Cang, C.; Giordana, C.; Monnerie, L.; Vandendriessche, J.; De Schryver, F. C. *Polymer* **1989**, 30, 45. (c) Jing, D. P.; Bokobza, L.; Monnerie, L.; Collart, P.; De Schryver, F. C. *Polymer* **1990**, 31, 110. (d) Bokobza, L. *Prog. Polym. Sci.* **1990**, 15, 337.
- (a) Guo, R. K.; Tazuke, S. *Macromolecules* **1989**, 22, 3286. (b) Tazuke, S.; Guo, R. K.; Ikeda, T.; Ikeda, T. *Macromolecules* **1990**, 23, 1208.
- Meyer, E. F.; Jamieson, A. M.; Simha, R.; Palmen, J. H. M.; Booij, H. C.; Maurer, F. H. J. *Polymer* **1990**, 31, 243.
- (a) Loutfy, R. O.; Law, K. Y. *J. Phys. Chem.* **1980**, 84, 2830. (b) Loutfy, R. O.; Arnold, B. A. *J. Phys. Chem.* **1982**, 86, 4205. (c) Loutfy, R. O.; Teegarden, D. M. *Macromolecules* **1983**, 16, 452. (d) Loutfy, R. O. *Pure Appl. Chem.* **1986**, 58, 1239.
- (a) Law, K. Y.; Loutfy, R. O. *Macromolecules* **1981**, 14, 587. (b) Law, K. Y.; Loutfy, R. O. *Polymer* **1983**, 24, 439.
- Anwand, D.; Müller, F. W.; Strehmel, B.; Schiller, K. *Makromol. Chem.* **1991**, 192, 1981.
- Dreger, Z. A.; Lang, J. M.; Drickamer, H. G. *Chem. Phys.* **1993**, 169, 351.
- (a) Fofana, M.; Veissier, V.; Viovy, J.-L.; Monnerie, L.; Johari, G. P. *Polymer* **1988**, 29, 245. (b) Fofana, M.; Veissier, V.; Viovy, J.-L.; Monnerie, L. *Polymer* **1989**, 30, 51. (c) Veissier, V.; Viovy, J.-L.; Monnerie, L. *Polymer* **1989**, 30, 1262.
- (a) Blackburn, F. R.; Cicerone, M. T.; Hietpas, G.; Wagner, P. A.; Ediger, M. D. *J. Non-Cryst. Solids* **1994**, 172–174, 256. (b) Blackburn, F. R.; Cicerone, M. T.; Ediger, M. D. *J. Polym. Sci., Polym. Phys. Ed.* **1994**, 32, 2595.
- Ehlich, D.; Sillescu, H. *Macromolecules* **1990**, 23, 1600.
- Deppe, D. D.; Torkelson, J. M. *Polym. Mater. Sci. Eng.* **1995**, 73, 338; manuscript submitted.
- Miller, K. E.; Krueger, R. H.; Torkelson, J. M. *J. Polym. Sci., Polym. Phys. Ed.*, in press; *Polym. Mater. Sci. Eng.* **1995**, 73, 555. See also the article on "Smart Polymers" in the Sept. 18, 1995, issue of *Chem. Eng. News*.
- Williams, M. L.; Landel, P. F.; Ferry, J. D. *J. Am. Chem. Soc.* **1955**, 77, 3701.
- (a) Angell, C. A. *J. Non-Cryst. Solids* **1988**, 103, 205. (b) *Ibid.* **1991**, 131–133, 13.
- Dhinojwala, A.; Wong, G. K.; Torkelson, J. M. *Macromolecules* **1992**, 25, 7395.
- Dhinojwala, A.; Hooker, J. C.; Torkelson, J. M. *J. Non-Cryst. Solids* **1994**, 172–174, 286.
- Matsuoka, S. *Relaxation Phenomena in Polymers*; Hanser Publishers: New York, 1992.
- McKusick, B. C.; Heckert, R. E.; Clairns, T. L.; Coffman, D. D.; Mower, H. F. *J. Am. Chem. Soc.* **1958**, 80, 2806.
- The lower  $T_g$  of the SHG samples, as compared to the fluorescence samples, originates from the slight plasticization due to higher levels of chromophore doping.  $T_g$  variations in the iBMA-based polymers most likely stem from differences in tacticity.
- Melhuish, W. H. *J. Opt. Soc. Am.* **1964**, 54, 183.
- Dhinojwala, A.; Hooker, J. C.; Torkelson, J. M. *ACS Symp. Ser.* **1995**, No. 601, 318.
- Meredith, G. R.; VanDusen, J. G.; Williams, D. J. *Macromolecules* **1982**, 15, 1385.
- Dhinojwala, A.; Wong, G. K.; Torkelson, J. M. *J. Opt. Soc. Am. B* **1994**, 11, 1549.
- Boyd, G. T.; Francis, C. V.; Trend, J. E.; Ender, D. A. *J. Opt. Soc. Am. B* **1991**, 8, 887.
- Levine, B. F.; Bethea, C. J. *J. Chem. Phys.* **1975**, 63, 2666.
- Dhinojwala, A. Ph.D. Thesis, Northwestern University, Evanston, IL, 1994.
- (a) Kohlrausch, R. *Ann. Phys. (Leipzig)* **1847**, 12, 393. (b) Williams, G.; Watts, D. C. *Trans. Faraday Soc.* **1970**, 66, 80.

- (42) Moynihan, C. T.; Eastel, A. J.; Tran, D. C.; Wilder, J. A.; Donovan, E. P. *J. Am. Ceram. Soc.* **1976**, *59*, 137.
- (43) (a) Patterson, G. D.; Stevens, J. R.; Lindsey, C. P. *J. Chem. Phys.* **1979**, *70*, 643. (b) Patterson, G. D.; Stevens, J. R.; Lindsey, C. P. *J. Macromol. Sci. Phys.* **1980**, *18*, 641.
- (44) (a) Roland, C. M.; Ngai, K. L. *Macromolecules* **1992**, *25*, 5765. (b) *Ibid.* **1993**, *26*, 6824; (c) *J. Non-Cryst. Solids* **1994**, *172-174*, 868.
- (45) As mentioned previously, this behavior has been noted in ref 30 for iBMA-based copolymers containing covalently attached Disperse Red 1 chromophores. Furthermore, the method by which  $\langle r \rangle$  is calculated, given in eq 4, appropriately weights the time components through its linear integration in time.
- (46) Ferry, J. D. *Viscoelastic Properties of Polymers*; John Wiley & Sons, Inc.: New York, 1980.
- (47) Dhinojwala, A.; Torkelson, J. M., manuscript in preparation.
- (48) Hamilton, K. H.; Miller, R. D.; Burland, D. M.; Torkelson, J. M., unpublished results.
- (49) Deshpande, A. V.; Beidoun, A.; Penzkofer, A.; Wagenblast, G. *Chem. Phys.* **1990**, *148*, 141.
- (50) Royal, J. S. Ph.D. Thesis, Northwestern University, Evanston, IL, 1992.
- (51) Also tested was the rotor probe 4-(tricyanovinyl)-*N,N*-diethylaniline (which is identical to the TC1 chromophore except for a hydrogen atom replacing the hydroxyl group in TC1). With this chromophore, the temperature dependence of the fluorescence in PiBMA was observed to be slightly less than that for the TC1 probe. This is consistent with the smaller chromophore motions being less coupled to the polymer relaxations. Another possible explanation is that the small degree of H-bonding between the hydroxyl group in the TC1 probe and the carbonyl group in PiBMA may result in slightly greater coupling of the TC1 rotor motions to the polymer and hence a slightly larger temperature dependence of its fluorescence. Such H-bonding effects have not been evidenced (outside experimental error) in a range of SHG studies investigating coupling of probe reorientation dynamics as a function of probe size and structure (See refs 40 and 47).
- (52) Parker, C. A. *Photoluminescence of Solutions*; Elsevier Publishing: Amsterdam, 1968.
- (53) (a) Doolittle, A. K. *J. Chem. Phys.* **1951**, *22*, 1031. (b) *Ibid.* **1951**, *22*, 1471.
- (54) In the case of the rotor probe 4-(tricyanovinyl)-*N,N*-diethylaniline tested only in PiBMA,  $\xi$  was found to be  $\sim 0.07$ , consistent with the values obtained for JMN and TC1.
- (55) Firestone, M. A.; Ratner, M. A.; Marks, T. J.; Lin, W.; Wong, G. K. *Macromolecules* **1995**, *28*, 2260.
- (56) Kulik, A. S.; Beckman, H. W.; Schmidt-Rohr, K.; Radloff, D.; Pawelzik, U.; Boeffel, C.; Spiess, H. W. *Macromolecules* **1994**, *27*, 4746.
- (57) Ishida, Y.; Yamafuji, K. *Kolloid-Z.* **1961**, *177*, 97.
- (58) McCrum, N. G.; Read, B. E.; Williams, G. *Anelastic and Dielectric Effects in Polymeric Solids*; Dover: New York, 1967.
- (59) Bartenev, G. M.; Lomovski, V. A.; Ovchinnikov, E. Y.; Karandashova, N. Y.; Tulinova, V. V. *Polym. Sci. (Russian)* **1993**, *35*, 1386.
- (60) These values of apparent activation energies are consistent with those determined for JMN in isotactic and syndiotactic poly(methyl methacrylate) by Loutfy and Teegarden (see ref 18c).
- (61) These studies reported at the Fall 1995 ACS Meeting (Hooker, J. C.; Torkelson, J. M. *Abstracts of Papers*, Poly 170) followed the approach described in refs 14b and c.
- (62) Hooker, J. C.; Royal, J. S.; Torkelson, J. M., manuscript in preparation.

MA9506896